Journal of Rock Mechanics and Geotechnical Engineering 13 (2021) 717–726

Contents lists available at ScienceDirect

Journal of Rock Mechanics and Geotechnical Engineering

journal homepage: www.jrmge.cn

Full Length Article

Validity of continuous-failure-state unloading triaxial tests as a means to estimate the residual strength of rocks

Gabriel Walton [a,*], Steven Gaines [b], Leandro R. Alejano [c]

[a] Department of Geology and Engineering Geology, Colorado School of Mines, Golden, CO, 80401, USA
[b] Natural Resources Canada, CanmetMINING, Ottawa, Ontario, K1A 1M1, Canada
[c] Department of Natural Resources and Environmental Engineering, Universidad de Vigo, Vigo, 36310, Spain

ARTICLE INFO

Article history:
Received 9 October 2020
Received in revised form
8 January 2021
Accepted 21 January 2021
Available online 27 February 2021

Keywords:
Residual strength
Continuous-failure-state testing
Compression testing
Brittle rock mechanics

ABSTRACT

The residual strength of rocks and rock masses is an important parameter to be constrained for analysis and design purposes in many rock engineering applications. A residual strength envelope in principal stress space is typically developed using residual strength data obtained from compression tests on many different specimens of the same rock type. In this study, we examined the potential for use of the continuous-failure-state testing concept as a means to constrain the residual strength envelope using a limited number of specimens. Specifically, cylindrical specimens of three rock types (granodiorite, diabase, and Stanstead granite) were unloaded at the residual state such that a full residual strength envelope for each individual specimen was obtained. Using a residual strength model that introduces a single new strength parameter (the residual strength index, or RSI), the results of the continuous-failure-state unloading tests were compared to conventionally obtained residual strength envelopes. Overall, the continuous-failure-state residual strength data were found to be consistent with the conventional residual strength data. However, it was identified that the primary factor limiting an accurate characterization of the residual strength for a given rock type is not the amount of data for a given specimen, but the variety of specimens available to characterize the inherent variability of the rock unit of interest. Accordingly, the use of continuous-failure-state testing for estimation of the residual strength of a rock unit is only recommended when the number of specimens available for testing is very limited (i.e. < 5).

1. Introduction

The residual strength of rocks and rock masses is an important parameter in many rock engineering areas, including longwall or block caving mining (Castro et al., 2017; Zhang et al., 2019), mine pillar design (Sinha and Walton, 2018), tunnel design (Alejano et al., 2009), and slope stability (Jaeger, 1971; Rao, 1996; Alonso and Pinyol, 2015; Tiwari and Latha, 2019; Renani and Martin, 2020). Generally, the residual strength is considered to be the stress level at which the yield strength stabilizes after having decreased from the peak strength as a consequence of accumulated damage. A rock, or rock mass, is said to be in its residual state when its yield strength is equal to the residual strength. In this state, the material is heavily damaged and broken into blocks or pieces such that the deformation process during further yielding occurs primarily through rearrangement of these blocks and pieces rather than through their breakage (Hobbs, 1966; Jaeger, 1969). It is for this reason that materials in their residual state maintain a constant residual strength with continued strain.

The residual strength of an intact rock specimen can be obtained based on the complete stress–strain curve obtained from a laboratory compression test. For most brittle rocks loaded under confining stresses encountered in typical engineering applications (i.e. typically confining stress $\sigma_3 < 50$ MPa), the stress–strain curve enters a period of weakening (often referred to as strain-softening) beyond its peak strength. The rate of post-peak strength loss as a function of axial strain typically demonstrates a gradual decrease until a stress plateau is attained (Hudson et al., 1972; Lockner et al., 1991). This stress plateau is considered to define the residual strength for an individual specimen (Krsmanovic, 1967; Crowder and Bawden, 2004).

* Corresponding author.
E-mail address: gwalton@mines.edu (G. Walton).
Peer review under responsibility of Institute of Rock and Soil Mechanics, Chinese Academy of Sciences.

https://doi.org/10.1016/j.jrmge.2021.01.009

Rocks in their residual state are broken into pieces, and their behavior is therefore somewhat similar to that of a coarse, angular aggregate (Rosengren and Jaeger, 1968; Walton, 2014). Specifically, the residual strength of rock is defined by minimal (or null) effective cohesion and high frictional strength and is highly sensitive to confining stress. As a result, the conventional approach for defining the complete residual strength envelope of a rock in principal stress space involves conducting triaxial tests at multiple confinements. Using this approach, several previous studies have been completed documenting the residual strength characteristics of various rocks (e.g. Mahmutoglu, 1998; Walton et al., 2019).

An alternative approach for determination of residual strength of rock relies on the concept of continuous failure state (or multiple-failure state) triaxial testing, first introduced by Kovari and Tisa (1975). The general idea is to modify the confining stress during a triaxial test according to some pre-defined criterion such that the failure (yield) surface of interest can be contacted at multiple different confining stress levels using a single rock specimen.

This concept has been widely applied for determination of the complete peak strength envelope using a single rock specimen (Kim and Ko, 1979; Kovari et al., 1983; Shimamoto, 1985; Youn and Tonon, 2010; Melati et al., 2014; Cammack and Duran, 2015; Ali et al., 2018; Minaeian et al., 2020). When using a multiple-failure state approach for determination of a peak strength envelope, several issues and challenges have been identified: (1) this method has been verified for some rock types, but its ability to accurately replicate multi-test strength envelopes varies from rock type to rock type (Kim and Ko, 1979); (2) the success of the method is dependent on the interpretation of the "imminent failure point" during testing, which is very difficult to determine (Youn and Tonon, 2010; Jin et al., 2018); and (3) the stress path selected and/or the development of damage during loading can lead to underestimation of subsequent peak strength values, particularly at later stages of loading as damage accumulates in the specimen (Melati et al., 2014; Cammack and Duran, 2015).

These challenges remain a barrier to the acceptance of such testing for estimation of the peak strength envelope in practice. When using the continuous failure state approach for evaluating residual strength envelope, however, the latter two concerns are much less significant, as the residual strength is effectively strain-history independent, meaning that determination of an exact point at which to change loading conditions is unnecessary.

The goal of this study is to evaluate the validity of applying the continuous failure state approach to the triaxial unloading phase of a compression test for determination of the residual strength envelope of a given rock type. To achieve this, we compared the results from triaxial tests with continuous failure state evaluation of the residual strength envelope during specimen unloading and the ones obtained using the conventional approach for residual strength determination. Three different rock types are considered. Additionally, the impact of unloading rate (one of the key testing parameters) on the obtained residual strength envelope is assessed and Monte Carlo simulation is presented to demonstrate the value-added of the continuous failure state testing approach when a limited number of specimens are available.

2. Methods

2.1. Rock types

This study considered three different rock types to demonstrate the general applicability of the proposed continuous failure state testing approach for residual strength determination: a granodiorite, a diabase, and Stanstead granite (see Fig. 1). While the residual strength data for these rocks have been previously reported as part of broader studies (Walton, 2018; Walton et al., 2019), these prior studies focused on the residual strength results obtained using the conventional approach and limited consideration was given to the continuous failure state data associated with the tests.

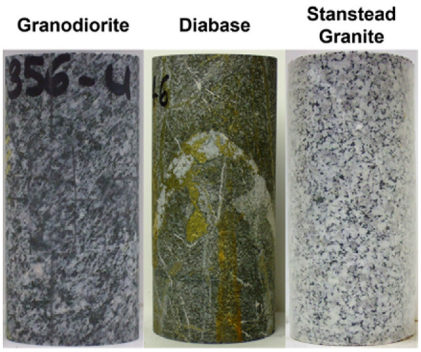

Fig. 1. Rock types considered in this study (modified from Walton et al., 2019).

The granodiorite presented in this study was collected from the Creighton Mine in Sudbury, Canada. Although no precise mineralogical analysis has been conducted, hand sample analysis suggests the rock is composed of approximately ~50% plagioclase felspar, ~25% quartz, ~20% biotite, and ~5% mafic minerals on average, with an average grain size of approximately 3 mm. It has an unconfined compressive strength (UCS) of approximately 185 MPa (±40 MPa).

The diabase presented in this study was collected from a deep copper deposit. The mineralogical composition of the diabase unit that was sampled is highly variable, but generally consists primarily of plagioclase feldspar (>50%) and pyroxene with variable amounts of sulphide minerals present (e.g. pyrite, chalcopyrite). Quartz veining is also present in the diabase unit, and these veins appear in some of the tested specimens (see Fig. 1). Note that these veins were not observed to consistently limit or lower specimen strength, as the veins themselves are strong relative to the rock matrix. The grain size of the diabase matrix is on the order of 1 mm, and the unit has a UCS of approximately 80 MPa (±40 MPa).

Stanstead granite is a well-studied granite from Quebec, Canada (Nasseri and Mohanty, 2008; Walton, 2018). Its typical composition is 33% plagioclase feldspar, 33% alkali feldspar, 25% quartz, and 9% micas, with grain sizes ranging from 0.5 mm to 2 mm. In this study, data for specimens from three separate blocks were tested; basic geomechanical results from the specimens obtained from the first two blocks have previously been reported (not including continuous failure state residual strength information) (Walton, 2018), while specimens obtained from the third block were tested specifically for the purposes of this study. While consistent differences in strength were observed between the different blocks (on the order of 10–15 MPa under unconfined conditions), these differences were typically small compared to the within-block variability (approximately ±10–15 MPa). Accordingly, the data from all three blocks were considered together in this study. The typical UCS of Stanstead granite is approximately 135 MPa (±30 MPa).

Granodiorite specimens had a diameter of 36 mm, diabase specimens had diameters of 43 mm or 63 mm, and Stanstead granite specimens were tested with multiple diameters (Block 1–43 mm, 63 mm, 75 mm; Block 2–81 mm, 101 mm; Block 3–54 mm, 81 mm). Specimens were cut to a length to diameter ratio of 2–2.25. The handling of these different specimen sizes in the interpretation of the test results is discussed in Section 3.

2.2. Testing procedure

All testing used to obtain the data for this study was conducted at the CanmetMINING Rock Mechanics Laboratory in Ottawa, Canada. Tests were conducted using a MTS Rock Mechanics Testing System, Model 815, using standard testing protocols as recommended by American Society of Testing Materials ASTM D7012-14 up to the point of unloading for continuous failure state determination of the residual strength envelope. Further details on the testing system, including technical specifications, are provided by Labrie and Conlon (2008). Axial displacements were recorded using linear variable differential transducers (LVDTs). Axial displacement control was used for all tests.

In a typical servo-controlled testing system, such as the MTS Model 815, two of the following variables are controlled and the other two are allowed to vary based on the rock specimen response to loading: axial displacement, confining stress, lateral displacement, and axial stress. In axial displacement controlled triaxial tests, the first two of these variables are controlled (axial displacement is increased at a constant rate and confining stress is held constant). The only distinction between a standard triaxial test procedure and the one used in these tests to obtain continuous failure state residual strength data is the addition of an unloading phase of testing after the residual strength is achieved. The unloading phase was commenced by the laboratory technician once the residual strength was deemed to have been attained per real-time monitoring of the axial stress–strain test data. During unloading, the confining pressure was gradually decreased while maintaining the same axial displacement rate used for the initial phase of the test; the application of these conditions in the servo-controlled system directly leads to a gradual reduction in the axial stress along the residual strength envelope such that the specimen is in a continuous state of yield (see Fig. 2). While most tests were conducted using an unloading rate of 0.1 MPa/s, a limited suite of tests on Stanstead granite were conducted with a variety of unloading rates to evaluate the influence of this parameter on the obtained residual strength results.

2.3. Data filtering

Peak strength was extracted from all triaxial tests, but not all tests were deemed to have reliable residual strength results, such as those shown in Fig. 3a. Specifically, in some cases, the technician running the test began the unloading phase of the test prior to reaching the residual strength (see Fig. 3b). Consideration of the axial stress level at the start of unloading in such cases may only introduce ~5–10% error into the residual strength estimate (for the data shown in Fig. 3b, the start of unloading was estimated to be ~7% higher than the residual strength plateau), which is not large relatively to the between-specimen variability in residual strengths. Nevertheless, to ensure a reliable comparison between conventional residual strength data and continuous failure state data, specimens that were visually assessed not to have reached the residual strength plateau prior to the start of unloading were filtered from the dataset prior to analysis.

In addition to filtering out potentially unreliable residual strength data based on the stress–strain curve itself, data were filtered based on examination of the unloading portion of the data in principal stress space. For example, if a given specimen did not achieve its residual strength prior to the onset of unloading, then its instantaneous yield strength envelope could be considered transient, and would be likely to evolve (further loss of strength) with continued axial straining during the unloading portion of the test. This phenomenon is illustrated in Fig. 4a. Fig. 4b shows an example of the unloading stress envelope obtained for a diabase specimen.

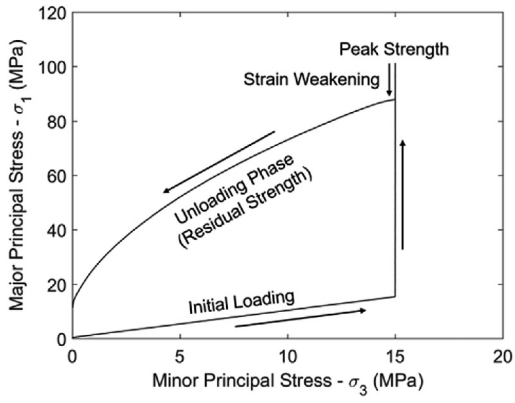

Fig. 2. Load path for continuous-failure state triaxial unloading tests.

Note the transition from one smooth yield envelope curve to another curve occurred around $\sigma_3 = 20$ MPa. Unsurprisingly, the likelihood of a strength transition being observed in the unloading data (indicating the specimen was not in its residual state when unloading began) was directly related to the degree to which the stress–strain curve suggested that the residual state may not have been achieved prior to unloading. Specimens deemed to be further from achieving the residual strength plateau, based on the stress–strain curve, tended to display more obvious strength drops in the unloading data.

Ultimately, the residual strength data considered in this study include those specimens deemed to be in the residual state prior to the start of unloading based on the stress–strain curve and that showed no evidence of a transition in yield envelopes in the unloading data. Note that the latter criterion was not considered in previous studies, so some specimens that were considered in previous studies (e.g. Walton et al., 2019) are not included in this study.

2.4. Modeling residual strength

The residual strength envelope of rock is nonlinear, which makes it potentially difficult to parametrize. Several nonlinear residual strength model formulations have been proposed (e.g. Cai et al., 2007; Peng and Cai, 2019; Walton et al., 2019), typically with some relation to the Hoek-Brown criterion. The use of such a model is necessary to enable comparison of results between conventional test data and continuous failure state unloading data. In this study, we apply the following model, which has been shown to perform similarly to or better than other models that introduce only one new parameter (Walton et al., 2019):

$$\sigma_1 = \sigma_3 + UCS\left(\frac{m_b}{UCS}\sigma_3\right)^a \tag{1}$$

$$m_b = m_i e^{\left(\frac{RSI-100}{28}\right)} \tag{2}$$

$$a = \frac{1}{2} + \frac{1}{6}\left[e^{\left(\frac{-RSI}{15}\right)} - e^{\left(\frac{-20}{3}\right)}\right] \tag{3}$$

where m_b and a are constants as per the generalized Hoek-Brown Criterion, m_i is the Hoek-Brown material constant for intact rock, and *RSI* stands for residual strength index, which is a constant that relates m_i to m_b and controls a. Note that Eq. (1) is equivalent to modeling the residual strength using the generalized Hoek-Brown criterion (after Cai et al., 2007) with the constant "*s*" term removed

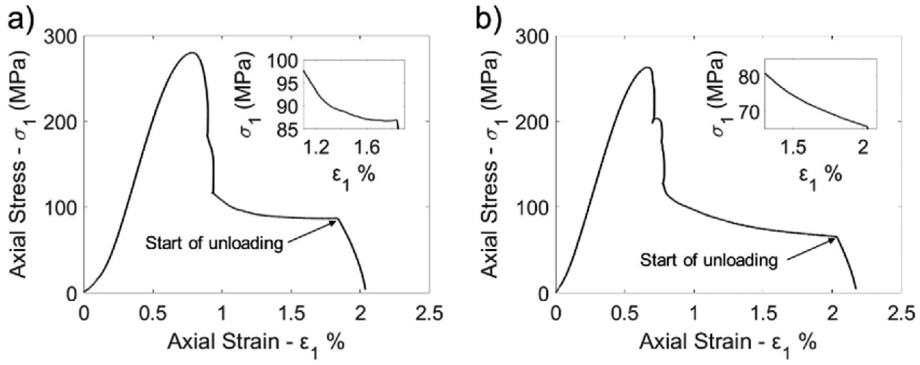

Fig. 3. Examples of two Stanstead granite specimens showing (a) a case tested at $\sigma_3 = 15$ MPa where residual strength was attained prior to unloading and (b) a case tested at $\sigma_3 = 15$ MPa where residual strength was not attained prior to unloading.

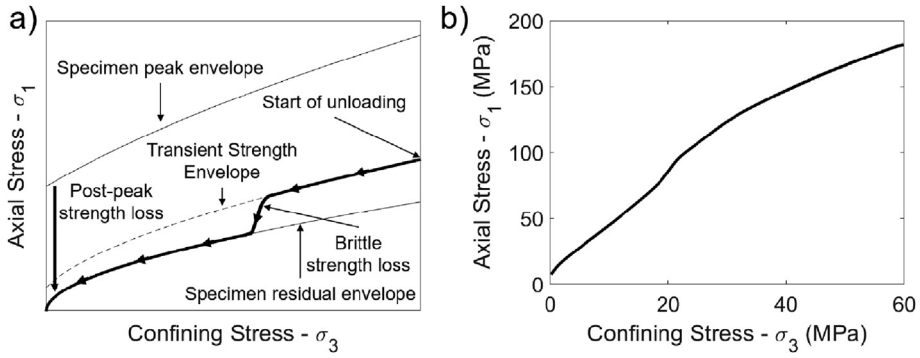

Fig. 4. Brittle strength loss during unloading – (a) schematic diagram; (b) example data from a diabase specimen tested at $\sigma_3 = 60$ MPa.

to force a zero residual strength under unconfined conditions (e.g. Walton et al., 2019). Eqs. (2) and (3) are equivalent to the originally proposed equations for estimation of m_b and a using geological strength index (GSI) (Hoek et al., 2002), with GSI being replaced by RSI. Although previous work has reported Eqs. (2) and (3) using the GSI terminology, this usage is not fully appropriate, as the absence of the "s" term in Eq. (1) changes the meaning of the fit parameter in Eqs. (2) and (3); this is reflected in the fact that the generalized Hoek-Brown criterion and Eq. (1) returns different fit parameter values (GSI vs. RSI, respectively) in the analysis by Walton et al. (2019).

Note that the model represented by Eqs. (1)–(3) can be fit to either conventional residual strength data (one strength point per test in principal stress space) or continuous failure state data using common least-squares fitting approaches. The authors acknowledge that the fact that Eqs. (1)–(3) forcing a residual strength of zero under unconfined conditions is a limitation of the proposed model. While zero residual strength under unconfined conditions is a reasonable physical expectation (i.e. purely "frictional" strength in the residual state), some laboratory studies have shown a (small) non-zero residual strength under unconfined conditions (e.g. Gowd and Rummel, 1980; Arzua and Alejano, 2013). Consideration of a non-zero residual strength under unconfined conditions in a residual strength model based on the generalized Hoek-Brown criterion would either require the addition of an "s" term determined based on RSI (i.e. based on the s estimation equation based on GSI of Hoek et al. (2002)) or the addition of a new, independent intercept fitting term. The former approach was not adopted in this study because it was previously found to perform similarly to or worse than the intercept-free model represented by Eqs. (1)–(3) in an examination of residual strength data from a wide variety of rocks (Walton et al., 2019). The latter approach was not adopted in this study because addition of an independent intercept parameter would add significant complexity to the model and complicate the interpretation and comparison of residual strength trends throughout the study.

2.5. Characterizing residual strength using continuous failure curves

Each continuous failure state test provides a complete residual strength envelope spanning from $\sigma_3 = 0$ MPa up to the confining stress at which the triaxial test in question was conducted. For each test with valid residual strength data (see Section 2.3), the unloading data were extracted, and the data corresponding to confining stress below double the unloading increment (i.e. 0.2 MPa for most tests based on an unloading rate of 0.1 MPa/s) were removed. The removal of these very low confining stress data was intended to avoid issues associated with challenges in servo-control of the confining stress near unconfined conditions. The remaining data were used to fit a least-squares residual strength model according to Eqs. (1)–(3) to obtain an RSI value characterizing the specimen's residual strength.

Fig. 5 shows two examples of residual strength data from the unloading phases of tests on granodiorite specimens. These examples illustrate typical characteristics of the unloading data: the model-data fit is very good (with almost all R^2 values being above 0.98); the unconfined residual strength implied by the trend of the data is notably non-zero, in contrast to the trends observed in conventional residual strength data and the prediction of Eq. (1); the curvature of the data tends to be slightly less than that implied by Eq. (3) (minimum a value of 0.5). The reasons for the subtle deviations of the unloading data from the trend predicted by the model (based on conventional data) are unknown. The primary

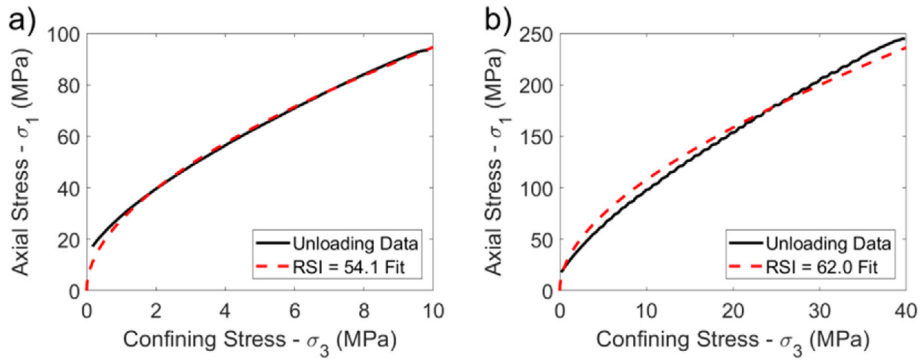

Fig. 5. Examples of model fits to unloading data from individual granodiorite triaxial tests conducted at (a) $\sigma_3 = 10$ MPa and (b) $\sigma_3 = 40$ MPa.

goal of this paper is to assess whether these slight differences in the residual strength envelope observed through continuous failure state testing lead to meaningful discrepancies in terms of results relative to those obtained using conventional data.

Although every specimen with continuous failure state unloading data for residual strength can be uniquely characterized by an individual RSI value, the practical goal of rock testing is typically to characterize an overall rock unit rather than an individual specimen. Accordingly, a method is necessary to combine information from multiple tests to characterize the rock unit as a whole. One simple approach is to take the mean or median RSI value from all the RSI values obtained for individual specimens. Given that the relationship between the RSI value and the underlying data is highly nonlinear, taking the mean or median of these fit parameter values may not be representative of the underlying trends. Accordingly, a second approach was also considered, wherein the unloading curve data for all specimens with valid data were compiled into a single data set that was used to fit a single RSI value. To avoid the data from specimens tested at higher initial confining stresses disproportionately influencing the fit, the curves were uniformly resampled to ensure an equivalent number of data points on each curve prior to fitting.

2.6. Monte Carlo uncertainty analysis

In the case of Stanstead granite, sufficient residual strength data ($n = 30$ specimens) were available to develop a well-constrained model of the "true" population residual strength using the conventional residual strength data; this is in contrast to the other two rock types, which had insufficient residual strength data ($n < 15$) to fully constrain the "true" population residual strength. For Stanstead granite, a Monte Carlo simulation with 20,000 realizations was performed to evaluate the potential range in results that might be obtained in estimation of the RSI of Stanstead granite when using either the conventional approach or the continuous failure state approach with different numbers of specimens. Specifically, for each possible number of specimens tested between 1 and 30 (the full data set), 20,000 combinations of specimens were randomly selected and the Stanstead granite RSI was evaluated from the conventional residual strength data and from the unloading data using the second approach described in Section 2.5 (fitting to all curves together). Based on the results of these simulations, the 95% prediction interval for the Stanstead granite RSI as obtained using the two different data types could be assessed for different numbers of test specimens. This analysis allowed for the determination of the relative amount of information added by considering unloading data in the assessment of residual strength rather than only considering one point per test.

3. Results

3.1. Granodiorite

The granodiorite triaxial test data (peak and residual) are shown in Fig. 6. The peak strength fit shown corresponds to $UCS = 185$ MPa and $m_i = 20.2$, while the conventionally obtained residual strength fit corresponds to an RSI value of 53.

Following determination of the individual test RSI values using the continuous failure state data, these values were plotted as a function of the initial confining stress of each of the tests (Fig. 7). These results demonstrate that there is no consistent bias in the residual strength results obtained as a function of confining stress. In other words, the confining stress used for a continuous failure state unloading test does not notably influence the residual strength result obtained. Much more significant, however, is the specimen-level variability, with specimens showing a residual strength above the conventional residual strength fit in Fig. 6, corresponding to higher RSI individual specimen RSI values in Fig. 7.

To obtain an overall RSI estimate for the granodiorite unit using the unloading data, a model was fit to all the unloading curves together. Fig. 8 shows the variability in the individual unloading curves, as well as a comparison between the conventionally obtained model (see Fig. 6) and the model fit to the unloading data. Overall, the models are very similar, predicting residual strengths within ~5% of each other at all confining stresses.

The results obtained by taking the mean and median of the individual test RSI values as well as using all the unloading data together (Fig. 8) are summarized in Table 1. Table 1 shows that the unloading results tend to underestimate the actual RSI of the granodiorite as estimated using the conventional residual strength data. This is believed in part to be associated with the slightly lower curvature of most of the unloading curves relative to the RSI model,

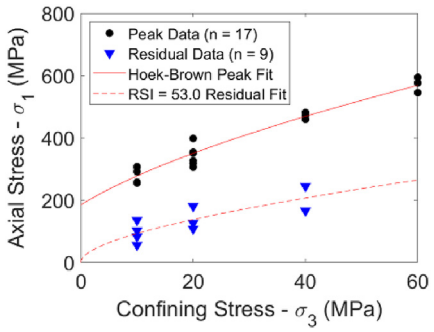

Fig. 6. Granodiorite peak and residual strength test data and associated fits.

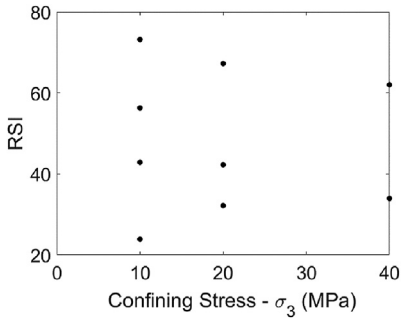

Fig. 7. Granodiorite RSI values derived from individual unloading curves as a function of confining stress.

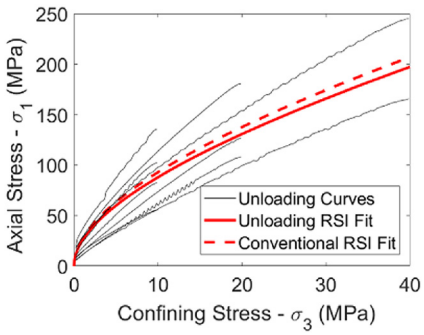

Fig. 8. Individual test unloading curves for granodiorite and associated RSI fit; the RSI fit obtained using the conventional residual strength data (one point per test) is shown for comparison.

as this means that the residual strength of an individual triaxial test at its initial confining stress tends to be slightly underestimated when fitting the RSI to the unloading data (see Fig. 5b). In the case of the RSI value obtained through fitting to all the unloading curves, this underestimation is relatively modest (a difference of −3.3 reported in Table 1 equivalent to a 6% underestimation), as is reflected in the fit comparison shown in Fig. 8. The greatest RSI underestimation occurs when using the median of the individual test RSI values to characterize the granodiorite unit; this significant underestimation occurs because the conventionally obtained RSI fit balances information from different tests using a least-squares regression, which is sensitive to extreme results, whereas the median is not influenced by such results. Overall, these results suggest that fitting a model to all the unloading curves together may be the best approach to characterize the RSI of a rock unit.

3.2. Diabase

The diabase triaxial test data (peak and residual) are shown in Fig. 9a. As noted in Section 2.1, the diabase specimens considered in this study included two different sizes (47 mm and 63 mm diameter). Given the relatively small discrepancy in specimen sizes, any potential size effect would be expected to be small (on the order of ~5%; Hoek and Brown, 1980), especially relative to the natural variability of the diabase, which is the most variable rock considered in this study. To evaluate any potential scale effects on the residual strength of the specimens, the conventional residual strength data were plotted separately and found to both follow the same overall trend (see Fig. 9b), which is consistent with the findings of previous studies for other rocks (e.g. Walton, 2018). Accordingly, the diabase data from both diameters were combined for the purposes of analysis. In Fig. 9a, the peak strength fit shown corresponds to $UCS = 77.7$ MPa and $m_i = 7.3$, while the conventionally obtained residual strength fit corresponds to an RSI value of 84.3.

As in the case of the granodiorite, individual test RSI values obtained using the continuous failure state data were evaluated as a function of the initial confining stress of each of the tests (Fig. 10). While these results tend to show no consistent trend at higher confining stresses, there is potential trend of lower RSI values occurring at lower confining stresses (no specimens show RSI < 75 for $\sigma_3 \geq 15$ MPa). An examination of Fig. 9b suggests that this may just be a coincidence, with the random variability in individual specimen strengths happening to cause lower-than-typical strength specimens that have been tested at lower confining stresses. Nevertheless, it appears that the individual test results may be more sensitive to such variations in specimen strength at lower confining stress than at higher confining stress.

To obtain an overall RSI estimate for the diabase unit using the unloading data, a model was fit to all the unloading curves together. Fig. 11 shows the variability in the individual unloading curves, as well as a comparison between the conventionally obtained model (see Fig. 9) and the model fit to the unloading data. As in the case of the granodiorite unit, the models are very similar, predicting residual strengths within ~5% of each other at all confining stresses.

The results obtained by taking the mean and median of the individual test RSI values as well as using all the unloading data together (Fig. 11) are summarized in Table 2. As in the case of the granodiorite results, Table 2 shows that the unloading results tend to underestimate the RSI value of the diabase as estimated using the conventional residual strength data. Again, the estimate closest to that obtained using the conventional data is provided by the model fit to all the unloading curves together.

3.3. Stanstead granite

The Stanstead granite data set used in this study is significantly larger than the granodiorite or diabase data sets. However, the Stanstead granite data includes specimens tested with a wide range of diameters (43 mm–101 mm). For the primary data analysis presented in this study to obtain as large a sample size as possible, all specimens of various diameters were considered together; this decision is justified on the basis that the scale effects influencing Stanstead granite peak strength are small relative to the between-specimen variability and, more importantly, the residual strength of Stanstead granite has previously been shown to be independent of specimen size (Walton, 2018). In addition to the tabulated results for the Stanstead granite unit as a whole, the final results are also shown for separate diameters to illustrate that the conclusions obtained by combining the various data sets together are similar to those obtained through analysis of each data set independently.

The Stanstead granite triaxial test data (peak and residual) for the complete data set are shown in Fig. 12. The peak strength fit shown corresponds to $UCS = 135.6$ MPa and $m_i = 31.1$, while the conventionally obtained residual strength fit corresponds to an RSI value of 35.2. Individual test RSI values obtained using the continuous failure state data are shown as a function of the initial confining stress of each of the tests in Fig. 13. As in the

Table 1
Summary of granodiorite RSI results obtained using unloading test data and their differences with respect to the conventionally obtained RSI estimate (53).

Item	Mean of individual values	Median of individual values	Fit to all unloading curves
RSI	48.2	42.9	49.7
Δ*RSI* relative to conventional value	−4.8	−10.1	−3.3

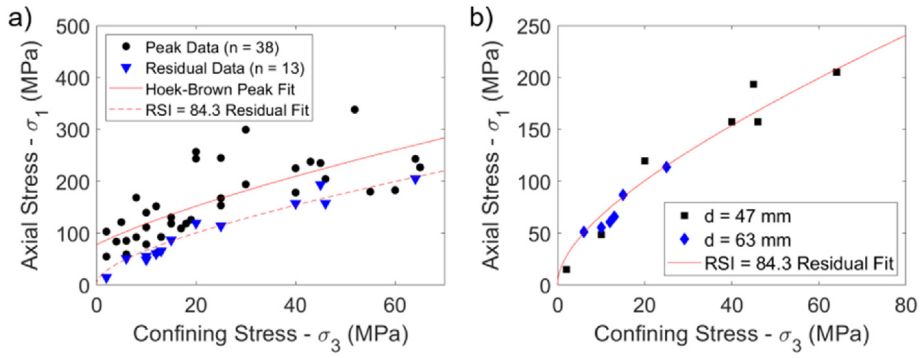

Fig. 9. (a) Diabase peak and residual strength test data and associated fits; and (b) zoomed view of the residual strength data illustrating a consistent trend independent of specimen diameter.

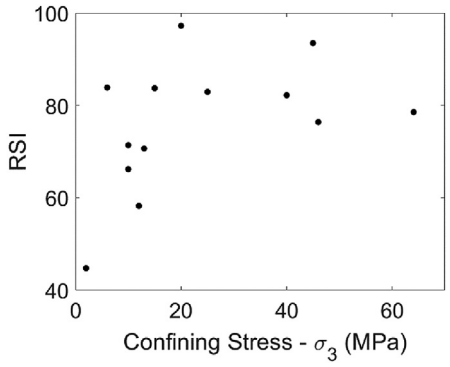

Fig. 10. Diabase RSI values derived from individual unloading curves as a function of confining stress.

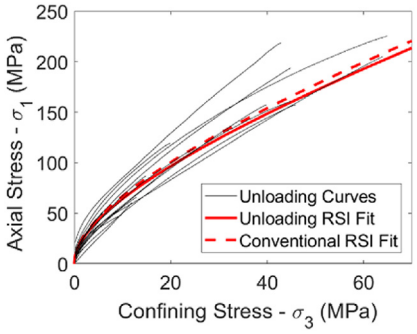

Fig. 11. Individual test unloading curves for diabase and associated RSI fit; the RSI fit obtained using the conventional residual strength data (one point per test) is shown for comparison.

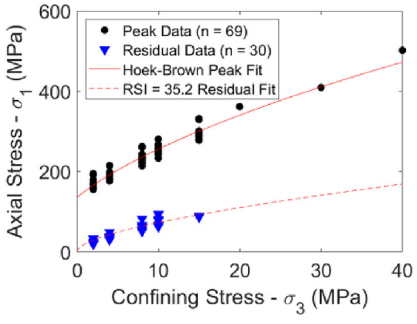

Fig. 12. Stanstead granite peak and residual strength test data and associated fits.

Table 2
Summary of diabase RSI results obtained using unloading test data and their differences with respect to the conventionally obtained RSI estimate (84.3).

Item	Mean of individual values	Median of individual values	Fit to all unloading curves
RSI	76.1	78.6	81.6
Δ*RSI* relative to conventional value	−8.2	−5.7	−2.7

case of the granodiorite results, the Stanstead granite results appear to be independent of the initial confining stress. To obtain an overall RSI estimate for Stanstead granite using the unloading data, a model was fit to all the unloading curves together. Fig. 14 shows the variability in the individual unloading curves, as well as a comparison between the conventionally obtained model (see Fig. 12) and the model fit to the unloading data. As was the case for the granodiorite and diabase, the models were very similar.

Table 3 presents a summary of the analysis results obtained when considering each of the data sets independently. Note that results from the most recently conducted test suite (third block in Section 2.1) were not included, as almost all of these tests were conducted at $\sigma_3 = 10$ MPa, making it difficult to properly constrain the complete Hoek-Brown envelope for the peak strength.

Table 4 summarizes the RSI results obtained using the unloading data when the Stanstead granite data are considered together. Overall, the Stanstead granite results are consistent with those obtained for the granodiorite and diabase units: the use of the unloading data tends to result in a slight underestimate of the actual RSI that characterizes the residual strength (per the conventional approach), and the approach whereby the RSI is estimated by fitting the residual strength model to all of the unloading curves together is the most appropriate manner for RSI estimation from unloading data. These conclusions are also generally consistent with the obtained from the smaller sub-samples of Stanstead granite studied for different diameters (Table 3), although these conclusions are not universal. For example, the RSI values obtained from the unloading data are not always lower than the conventionally obtained values (see results for $d = 63$ mm, $d = 75$ mm, and $d = 101$ mm). Furthermore, the fitting of the residual strength model to all the unloading data does not always result in the lowest error relative to the conventionally obtained RSI value (see results for $d = 81$ mm and $d = 101$ mm).

3.3.1. Evaluating the impact of unloading rate

One possible issue that was identified with respect to the testing procedure utilized for obtaining the continuous failure state

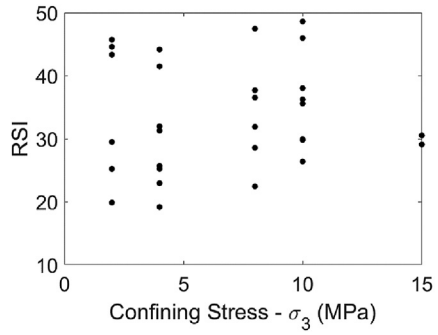

Fig. 13. Stanstead granite RSI values derived from individual unloading curves as a function of confining stress.

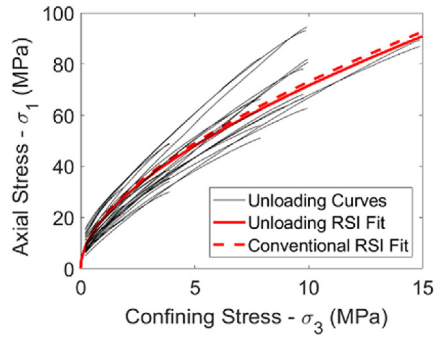

Fig. 14. Individual test unloading curves for Stanstead granite and associated RSI fit; the RSI fit obtained using the conventional residual strength data (one point per test) is shown for comparison.

residual strength data during unloading is that no standard exists for the unloading rate to be used. Although the CanmetMINING laboratory uses a rate of confining stress decrease of 0.1 MPa/s as their internal standard, the potential impact of this parameter on the residual strength results obtained using the unloading data has not been previously documented. To that end, some tests in the most recent test suite were conducted using unloading rates above and below the typical 0.1 MPa/s, setting $\sigma_3 = 10$ MPa as the initial confining stress with the intention of avoiding any potential confounding effects of modifying the initial confining stress. Following examination of the results shown in Fig. 13, which illustrates the independence of RSI on initial confinement, the tests with varying initial confining stresses were ultimately compiled together to evaluate the influence of unloading rate on the residual strength envelope obtained during unloading. These results are shown in Fig. 15.

Fig. 15 demonstrates that within the range of unloading rates considered (0.02 MPa/s to 0.2 MPa/s), the resulting residual strength data are not sensitive to the unloading rate used. Although this conclusion should be tested in future using additional data and for other rock types, it appears that an unloading rate of 0.1 MPa/s is indeed reasonable for the evaluation of residual strength through continuous failure state unloading.

Table 4
Summary of Stanstead granite RSI results obtained using unloading test data and their differences with respect to the conventionally obtained RSI estimate (35.2).

Item	Mean of individual values	Median of individual values	Fit to all unloading curves
RSI	33.5	31.6	34
Δ*RSI* relative to conventional value	−1.7	−3.6	−1.2

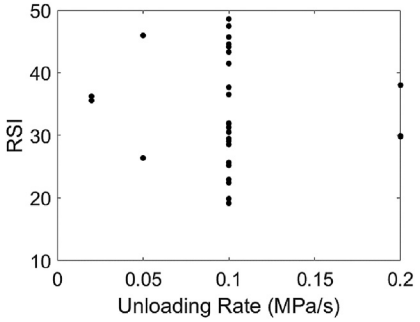

Fig. 15. Stanstead granite RSI values derived from individual unloading curves as a function of the confining stress unloading rate.

3.3.2. Monte Carlo uncertainty analysis

As described in Section 2.6, a 20,000 iteration Monte Carlo simulation was performed using random combinations of Stanstead granite specimens for several different numbers of specimens. The results of this analysis are shown in Fig. 16.

Fig. 16a compares the interval that bounds 95% of predicted Stanstead granite RSI cases for different numbers of test specimens when using either the conventional data (one data point per test) or the unloading data (with the approach of fitting the residual strength model to the data from all unloading curves together). These intervals are compared to the best estimate of the "true" population RSI for Stanstead granite as obtained from the full conventional residual strength data set ($n = 30$), as well as the 95% confidence intervals for that estimate (determined using MATLAB's fitnlm function; Mathworks, 2020). The first trend that can be observed in Fig. 16a is that the range in the calculated RSI values decreases as the number of specimens available for analysis increases; this is consistent with the general concept that as many tests as possible should be conducted to reflect the full range of

Table 3
Results obtained from analysis of Stanstead granite data sets by specimen diameter.

Item		Block 1			Block 2	
		$d = 43$ mm	$d = 63$ mm	$d = 75$ mm	$d = 81$ mm	$d = 101$ mm
Peak fit to triaxial data	*UCS* (MPa)	132.1	128.4	145.7	137.7	161.2
	m_i	26	29.8	25.1	29.2	30.2
Number of tests with valid residual strength data		8	5	3	4	2
RSI – conventionally obtained value		33.4	34.6	32.3	45.1	38.7
RSI – mean of individual values		30.2	33.4	34.7	44.2	39.2
RSI – median of individual values		31.4	34.1	28.8	45.2	39.4
RSI – fit to all unloading curves		32.2	34.7	32.4	43.8	39.4

variability in any rock mechanical parameter and to more accurately constrain a parameter value representative of the rock unit as a whole. The slight bias in the unloading results towards lower RSI values can also be observed. At lower numbers of specimens, this bias is partially counteracted by the smaller width of the unloading results interval (shown explicitly in Fig. 16b) such that the unloading data interval falls fully within the conventional data interval (see Fig. 16a).

Due to the slight tendency for the models fit to the unloading results to underestimate the true residual strength, it is clear that when a large number of specimens are available, conventional residual strength data should be used to evaluate a rock's residual strength envelope. However, it is important to determine whether or not the marginal benefit in terms of additional data for each specimen (see Fig. 16b) outweighs this disadvantage of the use of unloading data when smaller numbers of specimens are available. To answer this question, the percentage of cases in the Monte Carlo simulation where the RSI estimates obtained using the unloading data and the conventional data that fell within the 95% confidence interval for the "true" population average RSI for Stanstead granite was recorded for each number of specimens (Fig. 16c). As can be seen in Fig. 16c, when a relatively low number of specimens are considered (up to 8), it is more likely to obtain an RSI estimate for Stanstead granite between 31.9 and 38.6 (the 95% confidence interval) when using the unloading data than when using the conventional data. It should be noted that the benefit of using unloading data relative to conventional data is marginal, and that the number of specimens above which it becomes beneficial to use conventional data to constrain the residual strength will be smaller for rock types with a greater error in the unloading RSI relative to the conventional RSI (e.g. the granodiorite and diabase considered in this study).

The relatively small benefit in uncertainty reduction achieved by utilizing the continuous failure state unloading data (see Fig. 16b) was initially unexpected, as the unloading data provided a complete strength envelope to which a model can be fit rather than a single data point. This relatively small benefit of considering the full unloading envelope is attributed to two main factors: (1) the residual strength envelope obtained during unloading is largely constrained by the conventional residual strength value at the start of unloading, where with higher residual strength will both influence a conventional model fit towards higher RSI values and will also correspond to higher RSI unloading envelopes; (2) the model used to characterize the residual strength data is defined by a single previously unconstrained parameter (RSI; UCS and m_i are independently constrained by the peak strength data), meaning an RSI value for a given test can theoretically be established using a single data point (i.e. the conventional residual strength data). In other words, the primary factor limiting an accurate characterization of the residual strength for a given rock type is not the amount of data for a given specimen, but the variety of specimens that are available to characterize the inherent variability of the rock.

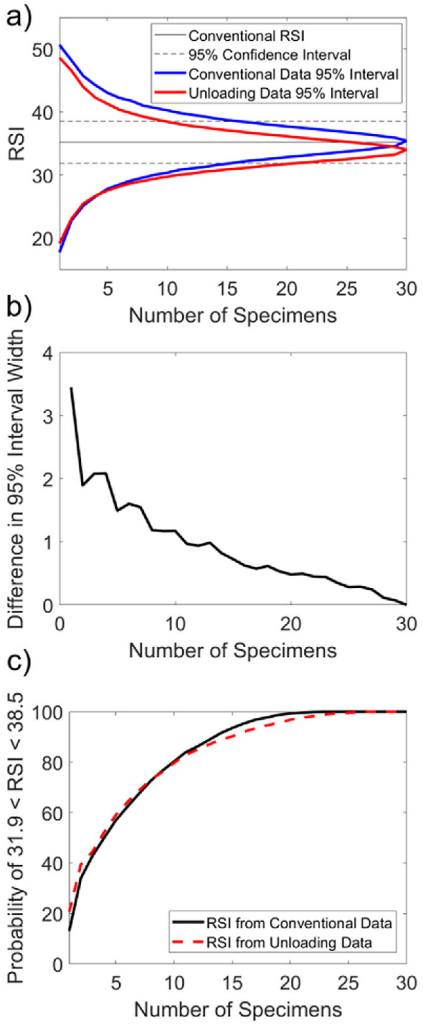

Fig. 16. Results of 20,000 simulations considering randomly sampled combinations of different numbers of test specimens – (a) Comparison of the intervals within which 95% of the calculated RSI values fall (using conventional and unloading data) with the 95% confidence interval for the "true" RSI of Stanstead granite as estimated using the full conventional data set ($n = 30$); (b) Reduction in the width of the calculated 95% RSI interval when using unloading data rather than conventional data for different numbers of specimens; (c) Probability of RSI estimates derived using unloading data or conventional data from different numbers of specimens falling within the 95% confidence interval for the "true" RSI of Stanstead granite as estimated using the full conventional data set ($n = 30$).

4. Conclusions

This study evaluated the validity of continuous failure state unloading testing as a means to characterize the residual strength of intact rock. Three rock types were considered (granodiorite, diabase, and Stanstead granite), and the residual strength results obtained using a conventional approach were considered as a reference against which the unloading test results were compared.

The primary conclusions of this study are as follows:

(1) Complete residual strength envelope data can be easily obtained on a specimen-by-specimen basis by unloading the confining stress applied to a specimen at a rate of 0.1 MPa/s, while maintaining a constant axial displacement rate.

(2) The residual strength, as characterized by a single residual strength index (RSI) parameter, was found to be generally consistent when evaluated using conventional data or continuous failure state unloading data. When using the unloading data and the proposed modeling approach, the residual strength is typically underestimated by a small amount (i.e. ~5% or less), although the results indicate that this is not a universal phenomenon (the residual strength may be slightly overestimated in some cases).

(3) The RSI as estimated using continuous failure state unloading data from individual specimens was generally found to be independent of the confining stress used for a triaxial test prior to the start of unloading.

(4) The main limiting factor in the accurate assessment of residual strength for a given rock unit was determined to be the number of specimens available to characterize the unit's geomechanical variability rather than the amount of data extracted from a given specimen. This finding also has potential implications for the use of multi-stage or continuous failure state testing in determination of other geomechanical parameters, such as peak strength.

(5) A Monte Carlo simulation was used to determine that the use of the continuous failure state unloading data to constrain the residual strength envelope of Stanstead granite was only preferable to the conventional approach when eight or less specimens were available for testing; more generally, the use of continuous failure state unloading tests for the characterization of residual strength is only recommended when an extremely small number of specimens is available (i.e. $n < 5$).

Declaration of competing interest

The authors declare that they have no known competing financial interests or personal relationships that could have appeared to influence the work reported in this paper.

Acknowledgements

The authors would like to acknowledge Denis Labrie, formerly of CanmetMINING (Ottawa, Canada), for his role in managing the testing campaigns through which the data for this paper were obtained. Ted Anderson and Gilles Brisson of CanmetMINING conducted the tests.

References

Alejano, L.R., Rodriguez-Dono, A., Alonso, E., Fdez-Manín, G., 2009. Ground reaction curves for tunnels excavated in different quality rock masses showing several types of post-failure behavior. Tunn. Undergr. Space Technol. 24 (6), 689–705.

Ali, S.S., Jin, G., Dhamen, A., Abdullah, A., Saad, B., 2018. Enhancing rock mechanical characterization-new approach to quantitatively determine the imminent failure state during multi-stage triaxial testing. In: Proceedings of the SPWLA 59th Annual Logging Symposium. London, UK. p. SPWLA-2018-FFF.

Alonso, E.E., Pinyol, N.M., 2015. Slope stability in slightly fissured claystones and marls. Landslides 12 (4), 643–656.

Arzúa, J., Alejano, L.R., 2013. Dilation in granite during servo-controlled triaxial strength tests. Int. J. Rock Mech. Min. Sci. 61, 43–56.

Cai, M., Kaiser, P.K., Tasaka, Y., Minami, M., 2007. Determination of residual strength parameters of jointed rock masses using the GSI system. Int. J. Rock Mech. Min. Sci. 44 (2), 247–265.

Cammack, R., Duran, A., 2015. A review of methods for assessing the hoek-Brown mi constant from triaxial testing. In: Proceedings of the 13th ISRM International Congress of Rock Mechanics. Montreal, Canada. p. ISRM-13CONGRESS-2015-010.

Castro, R.L., Basaure, K., Palma, S., Vallejos, J., 2017. Geotechnical characterization of ore related to mudrushes in block caving mining. J. S. Afr. Inst. Min. Metall 117 (3), 275–284.

Crowder, J.J., Bawden, W.F., 2004. Review of post-peak parameters and behaviour of rock masses: current trends and research. Rocnews. https://www.rocscience.com/documents/pdfs/rocnews/fall2004/Crowder_Bawden.pdf (Accessed 9 October 2020).

Gowd, T.N., Rummel, F., 1980. Effect of confining pressure on the fracture behaviour of a porous rock. Int. J. Rock Mech. Min. Sci. Geomech. Abstr. 17 (4), 225–229.

Hobbs, D.W., 1966. A study of the behaviour of a broken rock under triaxial compression, and its application to mine roadways. Int. J. Rock Mech. Min. Sci. Geomech. Abstr. 3 (1), 11–43.

Hoek, E., Brown, E.T., 1980. Underground Excavations in Rock. CRC Press.

Hoek, E., Carranza-Torres, C., Corkum, B., 2002. Hoek-Brown failure criterion-2002 edition. In: Proceedings of NARMS-TAC Conference, pp. 267–273.

Hudson, J.A., Crouch, S.L., Fairhurst, C., 1972. Soft, stiff and servo-controlled testing machines: a review with reference to rock failure. Eng. Geol. 6 (3), 155–189.

Jaeger, J.C., 1969. Behavior of closely jointed rock. In: Proceedings of the 11th US Symposium on Rock Mechanics (USRMS). Berkeley, California, USA. p. ARMA-69-0057.

Jaeger, J.C., 1971. Friction of rocks and stability of rock slopes. Geotechnique 21 (2), 97–134.

Jin, G., Ali, S.S., Al Dhamen, A.A., Saad, B., Hussain, M.G., Chinea, G., Nair, A., Alshanqaiti, E., 2018. Effect of various unloading criteria on rock failure parameters from multi-stage triaxial test - a comprehensive study. In: Proceedings of the 52nd U.S. Rock Mechanics/Geomechanics Symposium. Seattle, Washington, USA. p. ARMA-2018-1163.

Kim, M.M., Ko, H.Y., 1979. Multistage triaxial testing of rocks. Geotech. Test J. 2 (2), 98–105.

Kovári, K., Tisa, A., 1975. Multiple failure state and strain controlled triaxial tests. Rock Mech. 7 (1), 17–33.

Kovári, K., Tisa, A., Attinger, R.O., 1983. The concept of "continuous failure state" triaxial tests. Rock Mech. Rock Eng. 16 (2), 117–131.

Krsmanović, D., 1967. Initial and residual shear strength of hard rocks. Geotechnique 17 (2), 145–160.

Labrie, D., Conlon, B., 2008. Hydraulic and poroelastic properties of porous rocks and concrete materials. In: Proceedings of the 42nd U.S. Rock Mechanics Symposium (USRMS), San Francisco, California, USA. p. ARMA-08-182.

Lockner, D.A., Byerlee, J.D., Kuksenko, V., Ponomarev, A., Sidorin, A., 1991. Quasi-static fault growth and shear fracture energy in granite. Nature 350 (6313), 39–42.

Mahmutoglu, Y., 1998. Mechanical behaviour of cyclically heated fine grained rock. Rock Mech. Rock Eng. 31 (3), 169–179.

Mathworks, 2020. https://www.mathworks.com/help/stats/fitnlm.html (Accessed 9 October 2020).

Melati, S., Wattimena, R.K., Kramadibrata, S., Simangunsong, G.M., Sianturi, R.G., 2014. Stress paths effects on multistage triaxial test. In: Proceedings of the ISRM International Symposium-8th Asian Rock Mechanics Symposium. Sapporo, Japan. p. ISRM-ARMS8-2014-022.

Minaeian, V., Dewhurst, D.N., Rasouli, V., 2020. An investigation on failure behaviour of a porous sandstone using single-stage and multi-stage true triaxial stress tests. Rock Mech. Rock Eng. 53, 3542–3562.

Nasseri, M.H.B., Mohanty, B., 2008. Fracture toughness anisotropy in granitic rocks. Int. J. Rock Mech. Min. Sci. 45 (2), 167–193.

Peng, J., Cai, M., 2019. A cohesion loss model for determining residual strength of intact rocks. Int. J. Rock Mech. Min. Sci. 119, 131–139.

Rafiei Renani, H., Martin, C.D., 2020. Factor of safety of strain-softening slopes. J. Rock Mech. Geotech. Eng. 12 (3), 473–483.

Rao, S.M., 1996. Role of apparent cohesion in the stability of Dominican allophane soil slopes. Eng. Geol. 43 (4), 265–279.

Rosengren, K.J., Jaeger, J.C., 1968. The mechanical properties of an interlocked low-porosity aggregate. Geotechnique 18 (3), 317–326.

Shimamoto, T., 1985. Confining pressure reduction experiments: a new method for measuring frictional strength over a wide range of normal stress. Int. J. Rock Mech. Min. Sci. Geomech. Abstr. 22 (4), 227–236.

Sinha, S., Walton, G., 2018. A progressive S-shaped yield criterion and its application to rock pillar behavior. Int. J. Rock Mech. Min. Sci. 105, 98–109.

Tiwari, G., Latha, G.M., 2019. Reliability analysis of jointed rock slope considering uncertainty in peak and residual strength parameters. Bull. Eng. Geol. Environ. 78 (2), 913–930.

Walton, G., 2014. Improving Continuum Models for Excavations in Rockmasses under High Stress through an Enhanced Understanding of Post-yield Dilatancy. Ph.D. Thesis. Queen's University, Kingston, Canada.

Walton, G., 2018. Scale effects observed in compression testing of Stanstead granite including post-peak strength and dilatancy. Geotech. Geol. Eng. 36 (2), 1091–1111.

Walton, G., Labrie, D., Alejano, L.R., 2019. On the residual strength of rocks and rockmasses. Rock Mech. Rock Eng. 52 (11), 4821–4833.

Youn, H., Tonon, F., 2010. Multi-stage triaxial test on brittle rock. Int. J. Rock Mech. Min. Sci. 47 (4), 678–684.

Zhang, C., Tu, S., Zhao, Y.X., 2019. Compaction characteristics of the caving zone in a longwall goaf: a review. Environ. Earth Sci. Environ. Earth Sci. 78, 27.

Dr. Gabriel Walton obtained his Bachelors (2011) and PhD (2014) degrees in Geological Engineering from Queen's University, Canada. Since 2015, he has been employed as an Assistant Professor in the Department of Geology and Geological Engineering at the Colorado School of Mines. His work focuses on novel laboratory testing of rock properties, numerical modeling of underground excavations, and engineering applications of geophysics and remote sensing tools.